Accepted Manuscript

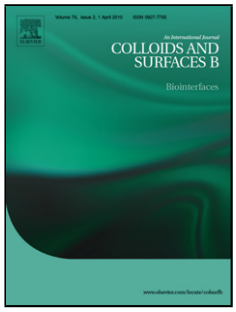

Title: Ruthenium bipyridine sensitized MoO_3 multifunctional nanostructures: Study of opto-electrochemical properties, biocompatibility and bioimaging

Authors: Murugan Veerapandian, Pramod K. Avti, V. Ravichandiran

PII: S0927-7765(17)30145-5
DOI: http://dx.doi.org/doi:10.1016/j.colsurfb.2017.03.029
Reference: COLSUB 8439

To appear in: *Colloids and Surfaces B: Biointerfaces*

Received date: 19-9-2016
Revised date: 18-2-2017
Accepted date: 12-3-2017

Please cite this article as: Murugan Veerapandian, Pramod K.Avti, V.Ravichandiran, Ruthenium bipyridine sensitized MoO3 multifunctional nanostructures: Study of opto-electrochemical properties, biocompatibility and bioimaging, Colloids and Surfaces B: Biointerfaceshttp://dx.doi.org/10.1016/j.colsurfb.2017.03.029

Ruthenium bipyridine sensitized MoO_3 multifunctional nanostructures: Study of opto-electrochemical properties, biocompatibility and bioimaging

Murugan Veerapandian[a,*], Pramod K. Avti[b,*], V. Ravichandiran[a]

[a]*National Institute of Pharmaceutical Education and Research, Kolkata 700032, West Bengal, India*

[b]*Department of Biophysics, Postgraduate Institute of Medical Education and Research, Sector-12 Chandigarh 160012, India*

*Corresponding authors

Dr. Murugan Veerapandian
DST-Inspire Faculty
Biomedical Nanotechnology Research Division
Department of Medicinal Chemistry
National Institute of Pharmaceutical Education and Research, Kolkata 700032,West Bengal, India
Email: momugan@gmail.com (M. Veerapandian),
Tel (Off): +91-033-24995803
Fax: +91-033-24187932

Dr. Pramod K. Avti
Assistant Professor
Department of Biophysics,
Postgraduate Institute of Medical Education and Research,
Sector-12, Chandigarh 160012, India
Email: pramod.avti@gmail.com, (P. Avti),
Tel (Off): +91-172-2755249.
Fax: +91-172-2744401

Graphical Abstract

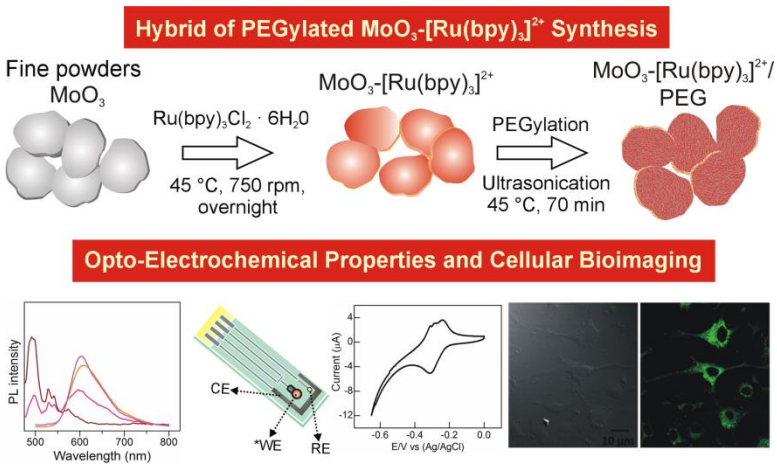

HIGHLIGHTS

- Fabrication of hybrid nanostructures of PEGylated MoO_3-$[Ru(bpy)_3]^{2+}$
- $[Ru(bpy)_3]^{2+}$ improves the opto-electrochemical properties of MoO_3 nanostructure
- Electrodes of MoO_3-$[Ru(bpy)_3]^{2+}$ exhibit amplified voltammetric properties
- PEGylation enhances the cellular biocompatibility of hybrid MoO_3-$[Ru(bpy)_3]^{2+}$

Abstract

Simple and versatile methodology to synthesis hybrid nanostructures with multi-functionality for device application is advantageous. Herein, we report the synthesis of MoO_3 nanostructures integrated with $[Ru(bpy)_3]^{2+}$ and PEGylation to obtain hybrid MoO_3-$[Ru(bpy)_3]^{2+}$ nanostructures. Chemically interacted $[Ru(bpy)_3]^{2+}$ provides optical and electrochemical properties to the hybrid structures. PEG_{3k} enhances the aqueous solubility of the hybrid system. Morphology, chemical structure, optical and electrochemical properties of hybrid nanostructures were studied from electron microscopic, spectroscopic and voltammetric techniques. The synthesized hybrid nanostructures exhibited a metal-to-ligand charge transfer absorbance and emission bands in the range of 450 nm and 605 nm, respectively. Electrode modified with MoO_3-$[Ru(bpy)_3]^{2+}$ and MoO_3-$[Ru(bpy)_3]^{2+}$/PEG_{3k} exhibit improved voltammetric properties than pristine MoO_3. Confocal cellular imaging supported that these hybrid particles were easily uptaken by endothelial cells with minimal cytotoxic effects. The hybrid nanocomplex displayed unique opto-electrochemical, cellular

biocompatibility and imaging features that may be an ideal platform for electrochemical biosensor devices with simultaneous bioimaging function.

Keywords: Molybdenum trioxide, $[Ru(bpy)_3]^{2+}$, Opto-electrochemical sensitizer, PEGylation, Cellular bioimaging

1. Introduction

Transition metal oxides such as molybdenum trioxide (MoO_3) is recently re-emerging as advanced functional material for various interdisciplinary applications *viz.,* photocatalysis [1], supercapacitors [2], electrochromics [3], sensors [4], additives in paints [5] and other biological applications [6]. Owing to its wide band gap (2.90 eV) semiconducting nature, high coloration efficiency and long-term thermochemical stability MoO_3 nanostructures are significantly explored for photochromic and thermochromic properties [1,7]. Very recently pristine MoO_3 nanoparticles and MoO_3 embedded polymer films have been investigated for anti-microbial applications [8,9]. Tran *et. al.,* demonstrated the potential cytotoxicity of chemically prepared MoO_3 nanoplates against invasive breast cancer iMCF7 cells [10]. Hybridization of metal oxide nanoparticles with optically and electrochemically active substances, through elemental doping and chemical conjugation, is the latest topic of interest potential for device construction (photo-electrochemical system) and biosensors [11]. Key factors influencing the development of advanced functional materials are appropriate choice of active constituents (inorganic or inorganic-organic complex), method of preparation and modification.

Efforts have been contributed in the development of novel composite structures based on MoO_3. For instance, He *et al.,* have prepared the Au nanoparticles spin-coated on the surface of MoO_3 thin films to obtain the enhanced UV photochromic effect [12]. Pt nanoparticles chemisorbed on MoO_x modified electrodes are established for electrochemical reduction of oxygen and its application in enzymatic glucose biosensor [13]. In addition to inorganic materials, organic polymer amalgamated with MoO_3 structure is also reported such as polyimide conjugated MoO_3 nanoflake as photocatalyst for hydrogen evolution from water under solar-light [14]. Highly ordered polyaniline on the interface layers of MoO_3 prepared by ion-exchange reaction in presence of dodecylamine, as an intercalator precursor, exhibited an enhanced electrical conductivity [15]. From these literature, it is apparent that functionalization of MoO_3 nanostructures using inorganic/organic components are potential strategy to create multifunctional applications.

Ruthenium bipyridine complex ($[Ru(bpy)_3]^{2+}$) is an amphiphilic molecule, with a three-dimensional spatial arrangement, composed of three bipyridine ligands binding to a metal Ru at the center. Due to its large Stokes fluorescence shift, quantum emission, enhanced thermal stability and electrochemical properties, $[Ru(bpy)_3]^{2+}$ dye complex is explored for functionalization of different metal/carbon nanostructures. For instance, $Ag@SiO_2$ and $Au@SiO_2$ for photocatalysis [16], Ag/chitosan for fluorescence quenching based biomolecular probing [17], graphene for electro-chemical and luminescence immunosensor [18,19]. In this context, hybridization of MoO_3 nanostructures with opto-electrochemically active inorganic-organic complex like $[Ru(bpy)_3]^{2+}$ is expected to provide multifunctional properties. Here, $[Ru(bpy)_3]^{2+}$ is used for the first time as an "opto-electrochemical sensitizer" on the surface of MoO_3 structures. Possible functionalization chemistry expected between microstructures of MoO_3 and $[Ru(bpy)_3]^{2+}$ are electrostatic, anion π-interactions and cation π-interactions. Fundamental changes in the optical absorbance, photoluminescence (PL), chemical structure and surface topography of MoO_3 functionalized $[Ru(bpy)_3]^{2+}$ (MoO_3-$[Ru(bpy)]^{2+}$) structures are studied with those of pristine MoO_3. The preliminary electrochemical properties of the different MoO_3-based nanostructure modified electrodes were studied to explore its further applicability in electrochemical biosensors. To enable the biocompatibility, functionalized composite structure was enriched with polyethylene glycol (PEG_{3K}, 3K represents M_w: 3000). Cytocompatibility of the resulted pristine MoO_3, MoO_3-$[Ru(bpy)_3]^{2+}$ and MoO_3-$[Ru(bpy)_3]^{2+}$/PEG were tested with brain endothelial cells, as *in vitro* model. Observed synergistic optical/electrochemical properties of MoO_3-$[Ru(bpy)_3]^{2+}$/PEG_{3k} with enriched biocompatibility enable their usefulness in multidisciplinary applications.

2. Experimental section

2.1 Synthesis of MoO_3 nanostructures

Nanostructures of MoO_3 were synthesized following the experimental protocol described in the literature [9], which is included in the section S1.2 of Supplementary material.

2.2 Surface modification of MoO_3 nanostructures with $[Ru(bpy)_3]^{2+}$

In a glass vial, 20 mg of MoO_3 powder and 20 mg of $Ru(bpy)_3Cl_2 \cdot 6H_2O$ was dissolved in 20 mL of DI H_2O:ethanol (1:1) mixture. The reaction vial is heated at 45 °C with a magnetically controlled stirring at 750 rpm for overnight, in dark environment. Reacted mixture containing particulate structures were separated by centrifugation at 8000 rpm for 20

min and washed twice with deionized (DI) water/ethanol. Isolated powders were redispersed in DI water for further investigation.

2.3 PEGylation of MoO_3-$[Ru(bpy)_3]^{2+}$ nanostructures

20 mg of MoO_3-$[Ru(bpy)_3]^{2+}$ powder and 40 mg of PEG_{3k} was dissolved in 20 mL of DI water and kept in ultrasonication bath with a setting temperature of 45 °C for 70 min. Afterward the reacted mixture is centrifuged (at 8000 rpm, 20 min), washed and utilized for further characterization.

2.4 Cell Culture

To understand the biocompatibility of the functionalized and non-functionalized MoO_3 nanostructures, brain endothelial cells (bEnd.3) were used as *in vitro* model system. Cells were cultured in Dulbecco's Modified Eagle's Medium (DMEM) supplemented with 10% fetal bovine serum (FBS) and incubated at 37^{o}C, and 5% CO_2 in a humidified atmosphere. Unless otherwise stated, all experiments were performed by seeding the cells at a density of 3×10^4 cells/cm^2.

2.5 Cell viability assay and confocal microscopic imaging

Cytocompatibility of the different nanostructures such as MoO_3, MoO_3-$[Ru(bpy)_3]^{2+}$ and MoO_3-$[Ru(bpy)_3]^{2+}$/PEG_{3k} were determined using the cell viability assay of bEnd.3 cells. Cells seeded in 96-well plates and after overnight incubation were treated with or without various concentrations of MoO_3 functionalized nanostructures for 12 h and 24 h duration. The concentrations for each material are varied from 0 to 100 µg/mL. Interference from the ligand conjugated MoO_3 species were assessed by addition of the assay reagents with the above concentration of MoO_3 particles but without cells. Cell viability was assessed using the Cell Titer 96 Aqueous One Solution Assay kit (G3580, Promega, WI, USA) according to the manufacturer instructions. Cell Titer solution (20 µL) was added to each well for 2 h and the plates were incubated at 37^{o}C and protected from light before making the measurements. The absorbance was recorded at 490 nm on microplate reader (BioTek Synergy 2, USA).

Cellular imaging was carried out using a LSM 710 Axio Observer confocal microscope (Carl Zeiss, Oberkochen, Germany) in the visible excitation wavelength of 458 nm. The fluorescence emissions were collected using a 560 nm long pass filter, to collect only $[Ru(bpy)_3]^{2+}$ emission beyond 560 nm [20]. The images were acquired at 24 h after the treatment with MoO_3-$[Ru(bpy)_3]^{2+}$ and MoO_3-$[Ru(bpy)_3]^{2+}$/PEG_{3k} using Plan Apochromatic 63 × 1.4 oil immersion objectives.

3. Results and discussion

Scheme 1 illustrates the overall synthesis and electrode processing of hybrid materials. Fine powders of MoO_3 structures are synthesized using the wet-chemical reaction of aqueous ammonium molybdate $(NH_4)_2MoO_4$ and HCl as precursor reagents. As-resulted precipitate of molybdic acid (H_2MoO_4) were purified and calcinated at 500 °C for 2 h to obtain the MoO_3 samples. Owing to its 2D lattice structures MoO_3 surfaces are convenient for functionalization reaction with $[Ru(bpy)_3]^{2+}$. Cationic metal center Ru^{2+} could react with MoO_3 species through electrostatic interaction. The existence of π-networks in the three bpy ligands could possibly mediate both cationic-π interactions and anionic-π interactions with MoO_3 *via* Mo^{x+} or Mo-O-Mo^{x+} and Mo=O^{-}, respectively. Relevant chemical structure analyses are discussed under FT-IR section. PEGylation of MoO_3-$[Ru(bpy)_3]^{2+}$ is achieved through ultrasonication, which supported the coating of PEG components on the surface of MoO_3-$[Ru(bpy)_3]^{2+}$. Acoustic microstreaming and cavitational bubbles from ultrasonication are known for coating the polymer layers on various nano/microstructures [21]. In this study, PEG moieties adsorbed on the surface of MoO_3-$[Ru(bpy)_3]^{2+}$ through intermolecular forces. Such PEGylated hybrid structures are useful for fabrication of biocompatible device discussed in the following sections.

Fig.1A shows the UV-vis absorbance of MoO_3 at 215 nm, ascribed to the charged inter band transition of $(MoO_6)^{6-}$ octahedrons mediated by the trapping electrons of $Mo^{6+} \leftrightarrow Mo^{5+}$ [9,22]. Aqueous $[Ru(bpy)_3]^{2+}$ exhibit the characteristic absorbance at 243, 285 and 450 nm attributed to the intra-ligand transition $\pi \rightarrow \pi^*$, bpy $\pi \rightarrow \pi_1^*$ transition and metal-to-ligand charge transfer (MLCT) bands of $[Ru(bpy)_3]^{2+}$, respectively [20]. Noticeable shoulder hump located at 420 nm is also corresponding to the MLCT (t_{2g} (Ru)-π^* (bpy) transitions). Upon interaction between the MoO_3 and dye $[Ru(bpy)_3]^{2+}$, significant changes were observed in the inherent transition bands of hybrid system. Notably, the inter band transitions of MoO_3 is not identified and the intra-ligand $\pi \rightarrow \pi^*$ transition of $[Ru(bpy)_3]^{2+}$ is diminished. Further, the intensity of bpy $\pi \rightarrow \pi_1^*$and MLCT bands were also significantly weakened with narrow peak width compared to the pristine dye. Observed changes in the individual peaks reveal the possible structural interactions between the two components and its influence in the optical properties.

Luminescence active hybrid materials are promising for optoelectronics and bioimaging applications [23]. Considering the optimal UV-vis absorbance of MoO_3 and MoO_3-$[Ru(bpy)_3]^{2+}$, herein, the PL emission properties were studied at an excitation

wavelength (λ_{ex}) of 220 and 450 nm (Fig. 1B). At 220 nm, pristine MoO_3 exhibit the characteristic PL emission bands, in the visible region, at 490, 530 and 540 nm attributed to the band-to-band transitions of distorted Mo-O and Mo-O-Mo crystal regions [24]. It has been designated that in addition to radiative recombination of electrons and holes, the oxygen vacancy defects at the surface of α-MoO_3 crystals are responsible for the visible emission peaks [25]. Similar to MoO_3, MoO_3-$[Ru(bpy)_3]^{2+}$ (excited at 220 nm) also exhibit the visible emission bands with a new peak centered at 605 nm, corresponded to the emission from the $[Ru(bpy)_3]^{2+}$, triplet MLCT excited state (^{3}MLCT) to ground state. PL spectra of $[Ru(bpy)_3]^{2+}$ and hybrid were also recorded at λ_{ex} of 450 nm which again ensured the standard emission due to ^{3}MLCT. Interestingly, the MoO_3-$[Ru(bpy)_3]^{2+}$ showed higher emission intensity (centered at 605 nm) than pristine dye molecules (at 610 nm). This perhaps attributed to the additional photoelectronic transitions derived from the oxygen vacancy site of MoO_3 and its inter-ligand transitions with the π-networks of bpy regions. Obtained PL results supported the optical evidence for the structural interaction within the hybrid MoO_3-$[Ru(bpy)_3]^{2+}$. Surface topographic analysis of MoO_3 samples from SEM revealed the presence of 2D nanosheet-like structures (Fig. S1), which were of ~500 nm long and 100–200 nm wide. Formation of sheet or plate like nanostructures of MoO_3 is perhaps due to the synthesis condition optimized in the thermal decomposition of molybdic acid into MoO_3 [5,9]. Upon reaction with $[Ru(bpy)_3]^{2+}$ and PEG molecules, the crystalline topography of nanostructures are observed to have smoothened surface, indicating the possible coating/functionalization (Fig. 1C).

ATR-FT-IR spectroscopy was used to study the chemical structure of individual samples (Fig. 2). MoO_3 samples exhibit the vibrations of (νMo–O) and (δMo–O) at 700 and 810 cm^{-1}, respectively. Bands observed at 840 and 985 cm^{-1} are corresponding to the stretching vibrations of oxygen atoms in Mo–O–Mo and Mo=O units, respectively [5]. Observed stretching modes support the layered orthorhombic α-MoO_3 phase [26]. $[Ru(bpy)_3]^{2+}$ modified MoO_3 samples showed distinct changes in the stretching and bending vibrations of Mo–O units located at 660, 705, 725 and 765 cm^{-1}. Further, stretching modes of oxygen in the Mo–O–Mo units appeared to have sharp peaks with minor shift at 845, 912 and 935cm^{-1}. Group frequencies located in the region 1370 to 1468 cm^{-1} are ascribed to the (νC=N) of bipyridine, supporting the chemical bonding of bpy ligands with MoO_3, *via* anion π-interactions/cation π-interactions. PEGylated MoO_3–$[Ru(bpy)_3]^{2+}$ samples are also studied to have group frequencies corresponded to Mo–O and Mo–O–Mo units with minor changes in peaks at 704, 760, 840, 900 and 935 cm^{-1}. Compared to MoO_3-$[Ru(bpy)_3]^{2+}$, PEGylated samples

exhibit moderate-to-weak signals from (νC=N) of bpy ligand. This result is perhaps due to the surface modification of PEG_{3k} species, which is evidenced from the distinct C-O stretching vibrations at 1635 cm^{-1}. Existence of C-O stretching might occur as a result of hydrolysis followed by oxidation of PEG moieties [27]. This peak is typical and not observed in other two samples, suggesting the successful PEGylation on MoO_3–$[Ru(bpy)_3]^{2+}$.

Cyclic voltammetric studies were carried out to assess the electrochemical properties and its associated molecular interaction of pristine MoO_3 and hybridized MoO_3 nanostructures, using methylene blue (MB) as redox mediator. The cyclic voltammograms (CVs) measured from three electrodes are shown in Fig. 3A. The MoO_3 nanostructures modified electrode exhibited a pair of well-resolved redox wave with an anodic and a cathodic peak potentials at –0.25 V and at –0.31 V, respectively, attributed to oxidation-reduction reaction of MB [28]. In addition to inherent anodic peak of MB, MoO_3-$[Ru(bpy)_3]^{2+}$ modified electrodes exhibited two additional anodic peaks at –0.32 V and –0.29 V, which perhaps related to the oxidation of $Ru^{2+}\rightarrow Ru^{3+}$ component exist in the hybrid system. Similarly, PEGylated MoO_3-$[Ru(bpy)_3]^{2+}$ modified SPE electrodes enabled the anodic peaks at –0.30 V and –0.28 V. It can be observed that the redox peak current intensities generated from MoO_3-$[Ru(bpy)_3]^{2+}$ and MoO_3-$[Ru(bpy)_3]^{2+}$/PEG_{3k} electrodes are comparatively better than pristine MoO_3. This result is ascribed to the synergistic electron-transfer property originated from Ru functionalization. Further, a scan rate dependent CV study (Fig. 3B) of MoO_3-$[Ru(bpy)_3]^{2+}$/PEG electrodes are measured to validate the linear relationship with increase of redox response.

The corresponding linear fit for three anodic peaks (I_{pa}) and one cathodic peak (I_{pc}) currents with scan rate provided a correlation coefficient of 0.9920 ($I_{pa}1$), 0.9950 ($I_{pa}2$), 0.9833 ($I_{pa}3$) and 0.9880 (I_{pc}), respectively, suggesting a surface-confined reaction at the interface. Due to the PEGylation process the final hybrid enabled a broadened anodic peak with no significant improvement in current intensities compared to pristine MoO_3-$[Ru(bpy)_3]^{2+}$. This might be due to the active barrier layers created by the PEG molecules on the surface of inherent MoO_3-$[Ru(bpy)_3]^{2+}$. Development of novel hybrid structures with retained inherent electrochemical properties is indeed promising for biomedical device, like biosensor platform.

Cell viability using MTS assay was performed to evaluate the biocompatibility of MoO_3, MoO_3-$[Ru(bpy)_3]^{2+}$ and MoO_3-$[Ru(bpy)_3]^{2+}$/PEG_{3k}. The results suggests that treatment with MoO_3 and MoO_3-$[Ru(bpy)_3]^{2+}$ shows no cytotoxicity up to 75 μg/ml for 12 h

whereas PEGylated MoO_3-$[Ru(bpy)_3]^{2+}$ further sustains viability up to 100 μg/ml for 12 h. Treatment of MoO_3 and MoO_3-$[Ru(bpy)_3]^{2+}$ for 24 h with 50 μg/ml and beyond decreased the cell viability to almost 50% whereas, the PEGylated MoO_3-$[Ru(bpy)_3]^{2+}$ had no statistical significant cytotoxic effect up to 100 μg/ml at 24 h. This clearly shows that unlike the pristine MoO_3 or its Ru complexed particles the PEGylated ones showed least cytotoxic effect and are more biocompatible. To further evaluate the cellular uptake of these biocompatible nanostructures, confocal fluorescence microscopic study was performed.

The cells treated with MoO_3-$[Ru(bpy)_3]^{2+}$ and the PEGylated MoO_3-$[Ru(bpy)_3]^{2+}$ were excited around 450 nm and the fluorescence cellular images were acquired beyond 560 nm using a long pass filter. Confocal images suggests that the MoO_3-$[Ru(bpy)_3]^{2+}$ are uptaken by the cells to a lesser extent still maintaining the cellular morphology (Fig. 4B[I, overlay image]). On the other hand the PEGylated MoO_3-$[Ru(bpy)_3]^{2+}$ (Fig. 4B[II, overlay image]) shows no changes in the cell morphology after their uptake. It could be assumed that most of the MoO_3-$[Ru(bpy)_3]^{2+}$ interact with the serum proteins present in the cell treated medium and form large nanoparticle aggregates that limit their cellular uptake unlike the PEGylated hybrid. This clearly explains the biocompatibility of MoO_3-$[Ru(bpy)_3]^{2+}$/PEG_{3k} as compared to MoO_3-$[Ru(bpy)_3]^{2+}$. Recently, it has been shown that PEGylated MoO_3 nanospheres synthesized have been employed as effective drug delivery and chemotherapeutic agents [29]. In another study, MoO_3 nanoparticles were used as intrinsic biomimetic for the sulfite oxidase activity under physiological conditions, a mitochondrial located molybdenum-containing enzyme was used in the detoxification process in the amino acid and lipid metabolism [30]. In this study, we have shown that the interaction between the MoO_3 and the $[Ru(bpy)_3]^{2+}$ helps acquiring the promising fluorescence imaging in the visible wavelengths covering ~550 nm to 700 nm through the standard emission due to ^{3}MLCT. The PEGylation helps in the cellular biocompatibility and uptake of nanoparticles and the preserved PL spectral properties are potential for cellular imaging. Such optical- and redox-active biocompatible hybrid material is expected to retain the inherent biological activity of immobilized antibody/peptide/nucleic acids and perhaps promising for development of multifunctional sensor probe based on fluorescence and electrochemistry.

4. Conclusion

Hybrid nanostructures of MoO_3 integrated $[Ru(bpy)_3]^{2+}$ surface modified with PEG molecules were synthesized successfully. MoO_3 nanoparticles with functional groups of Mo^{x+} or Mo-O-Mo^{x+} and $Mo{=}O^{-}$ exhibit the layered orthorhombic α-MoO_3 phase, which supported

the chemical interaction with $[Ru(bpy)_3]^{2+}$ *via* cationic-π and anionic-π interactions, respectively. Ultrasonication derived microstreaming and cavitational forces mediated the intermolecular interaction of PEG_{3K} species on the surface of MoO_3-$[Ru(bpy)_3]^{2+}$ through hydrolysis reaction. PEGylation not only promoted the solubility but also enriched the cellular biocompatibility of the developed hybrid nanostructures. UV-vis absorbance and emission properties of $[Ru(bpy)_3]^{2+}$ sensitized the optical properties of MoO_3 structures. Functionalization of $[Ru(bpy)_3]^{2+}$ show significant improvement in the electrochemical properties of MoO_3. Developed procedure enhances the facile incorporation of multiple functional groups for obtaining the desired opto-electrochemical and bioimaging properties in single platform. Additional studies could improve the features of hybrid structure on electrode interface, advantageous for construction of biosensors toward variety of biomedical applications.

Acknowledgments

M. Veerapandian acknowledges the support of Department of Science and Technology, India for the DST-Inspire Faculty award (DST/INSPIRE/04/2015/002081). Authors would like to thank Prof. Suresh Neethirajan, Director, BioNano Lab, University of Guelph, ON, Canada for the support.

References

[1] L. Cheng, M. Shao, X. Wang, H. Hu, Chem. Eur. J. 15 (2009) 2310.

[2] M. Sarfraz, M.F.A. Aboud, I. Shakir, J. Alloy. Compd. 650 (2015) 123.

[3] N.A. Chernova, M. Roppolo, A.C. Dillon, M.S. Whittingham, J. Mater. Chem. 19 (2009) 2526..

[4] P. Song, Q. Wang, J. Li, Z. Yang, Sens. Actuat. B-Chem 181 (2013) 620.

[5] K. Krishnamoorthy, M. Premanathan, M. Veerapandian, S.J. Kim, Nanotechnology 25 (2014) 315101.

[6] A. Fakhri, P.A. Nejad, J. Photochem. Photobiol. B 159 (2016) 211.

[7] S.A. Tomas, M.A. Arvizu, O. Zelava-Angel, P. Rodriguez, Thin Solid Films, 518 (2009) 1332.

[8] C. Zollfrank, K. Gutbrod, P. Wechsler, J.P. Guggenbichler, Mater. Sci. Eng. C 32 (2012) 47.

[9] K. Krishnamoorthy, M. Veerapandian, K.S. Yun, S.J. Kim, Colloid. Surface B. 112 (2013) 521.

[10] T.A. Tran, K. Krishnamoorthy, Y. W. Song, S. K. Cho, S. J. Kim, ACS Appl. Mater. Interfaces 6 (2014) 2980.

[11] Y. Li, X. Yang , Y. Feng , Z. Yuan, B. Su, Crit. Rev. Solid State, 37 (2012) 1.

[12] T. He, Y. Ma, Y. Cao, P. Jiang, X. Zhang, W. Yang, J. Yao, Langmuir17 (2001) 8024.

[13] I. Cakar, K.V. Ozdokur, B. Demir, E. Yavuz, D.O. Demirkol, S. Kocak, S. Timur, F.N. Ertas, Sens. Actuat. B-Chem. 185 (2013) 331.

[14] C. Maa, J. Zhou, Z. Cui, Y. Wang, Z. Zou, Sol. Energ. Mat. Sol. C. 150 (2016) 102.

[15] Y. Li, Y. Xiang, X. Dong, J. Xu, F. Ruan, Q. Pan, J. Solid State Chem. 182 (2009) 2041.

[16] K. Mori, M. Kawashima, M. Cheand and H. Yamashita, Angew. Chem. Int. Ed. 49 (2010) 8598.

[17] M. Veerapandian, X.X. Zhu and S. Giasson, J. Mater. Chem. B 3 (2015) 665.

[18] F.N. Xiao , M. Wang, F.B. Wang, X.H. Xia, Small, 10 (2014) 706.

[19] M. Veerapandian, S. Neethirajan, RSC Adv. 5 (2015) 75015.

[20] P.K. Avti, B. Sitharaman, Int. J. Nanomedicine. 7 (2012) 1953.

[21] M. Veerapandian, K.S. Yun, Polym. Composite. 31 (2010) 1620.

[22] H. Sinaim, A. Phuruangrat, S. Thongtemc, T. Thongtem, Mater. Chem. Phys. 132 (2012) 358.

[23] C. Zhang, J. Lin, Chem. Soc. Rev. 41 (2012) 7938.

[24] I. Navas, R. Vinodkumar, V.P. Mahadevan Pillai, Appl. Phys. A. 103 (2011) 373.

[25] L.X. Song, J. Xia, Z. Dang, J. Yang, L.B. Wang, J. Chen, Cryst. Eng. Comm. 14 (2012) 2675.

[26] A. Klinbumrung, T. Thongtem, S. Thongtem, J. Nanomater. 930763 (2012) 1.

[27] G.D. Venkatasubbu, S. Ramasamy, G.S. Avadhani, V. Ramakrishnan, J. Kumar, Powder Technol. 235 (2013) 437.

[28] D. Zhang, L. Fu, L. Liao, B. Dai, R. Zou, C. Zhang, Electrochim. Acta 75 (2012) 71.

[29] T. Bao, W. Yin, X. Zheng, X. Zhang, J. Yu, X. Dong, Y. Yong, F. Gao, L. Yan, Z. Gu, Y. Zhao, Biomaterials 76 (2016) 11.

[30] R. Ragg, F. Natalio, M.N. Tahir, H. Janssen, A. Kashyap, D. Strand, S. Strand, W. Tremel, ACS Nano 8(5) (2014) 5182.

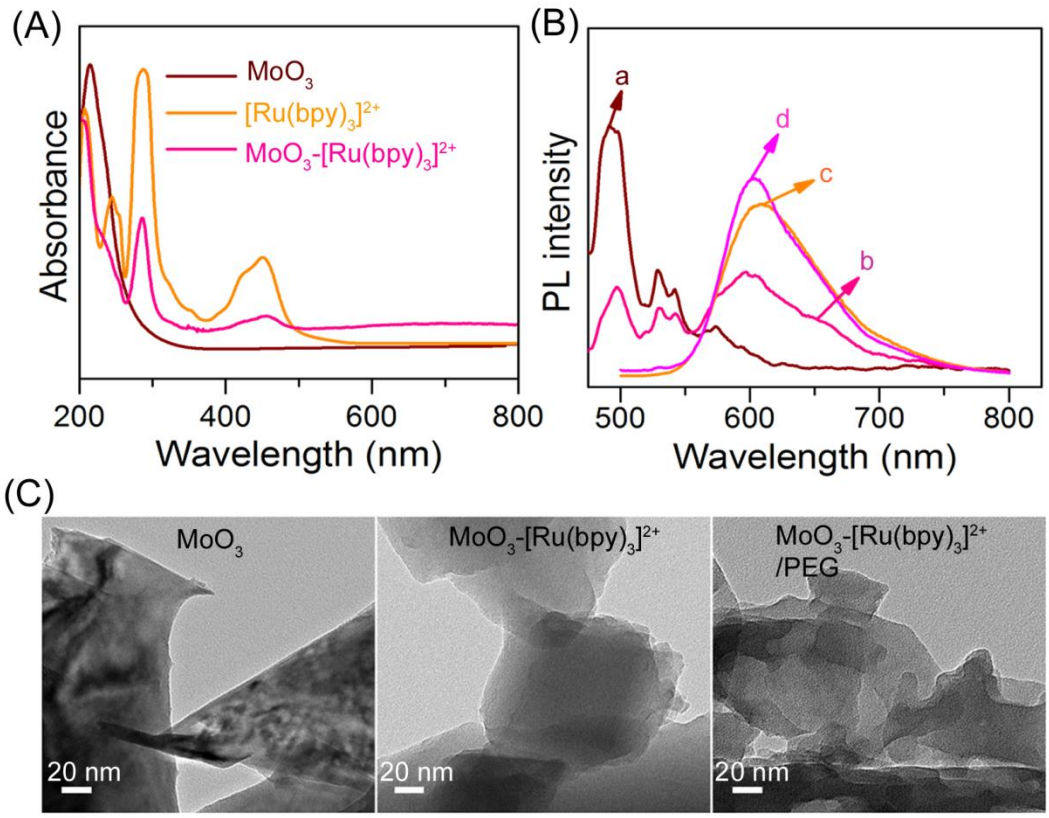

Fig. 1. (A) UV-visible absorbance spectra, (B) photoluminescence spectra of (a) MoO_3 and (b) MoO_3-$[Ru(bpy)_3]^{2+}$ at an excitation wavelength (λ_{ex}) of 220 nm, (c) $[Ru(bpy)_3]^{2+}$ and (d) MoO_3-$[Ru(bpy)_3]^{2+}$ at λ_{ex} of 450 nm. (C) HR-TEM images.

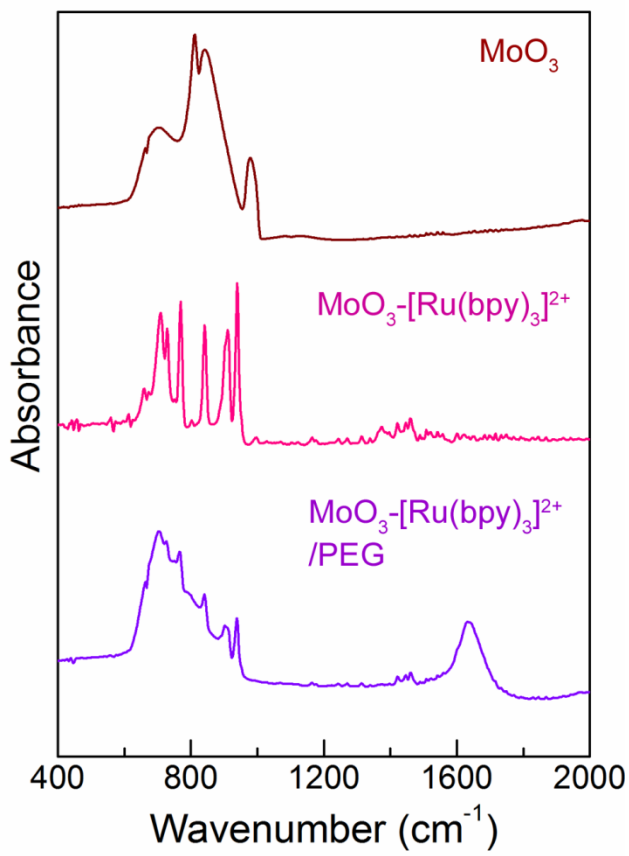

Fig. 2. ATR-FTIR spectra of MoO_3, MoO_3-$[Ru(bpy)_3]^{2+}$ and MoO_3-$[Ru(bpy)_3]^{2+}$/PEG_{3k} powder samples.

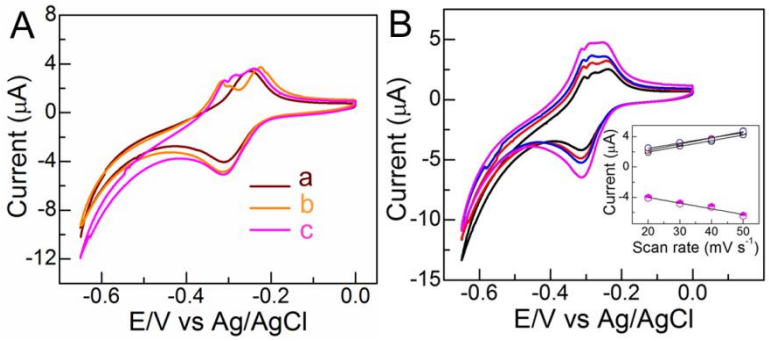

Fig. 3. CVs of (a) MoO_3, (b) MoO_3-$[Ru(bpy)_3]^{2+}$ and (C) MoO_3-$[Ru(bpy)_3]^{2+}$/PEG_{3k} modified SPE electrodes measured in 10 mM PBS (pH 7.4) supported with MB (0.5 mg/mL), scan rate 30 mV/s. (B) CVs of MoO_3-$[Ru(bpy)_3]^{2+}$/PEG_{3k} modified SPE electrode at different scan rates (20-50 mV/s) in 10 mM PBS (pH 7.4) supported with MB (0.5 mg/mL). Inset shows the corresponding plots of the anodic and cathodic peak currents versus scan rates.

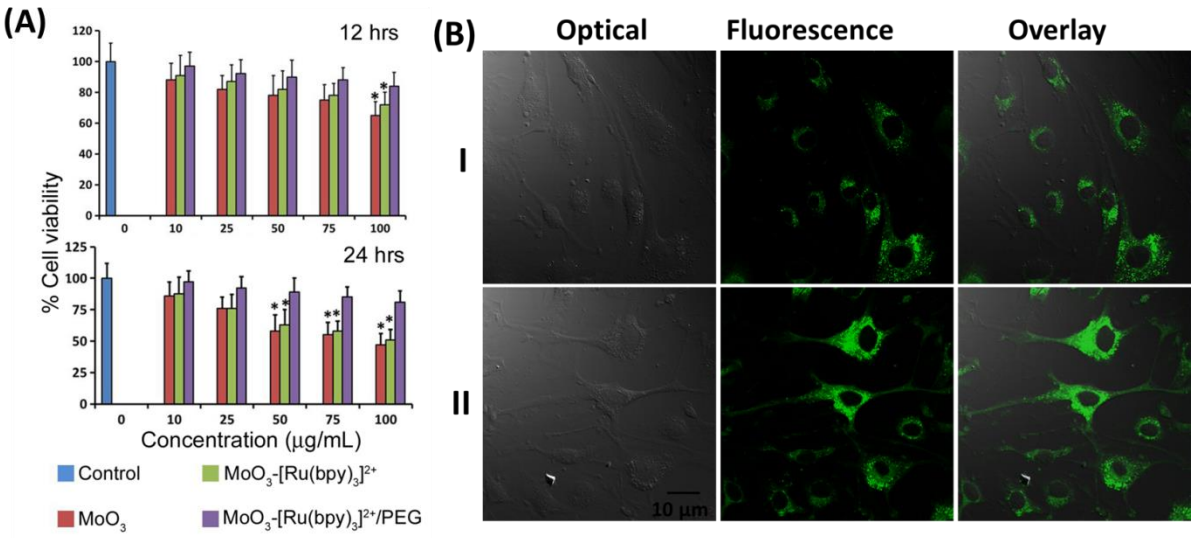

Fig 4. (A) Effects on bEnd.3 cells viability at different concentrations of MoO_3, MoO_3-$[Ru(bpy)_3]^{2+}$ and MoO_3-$[Ru(bpy)_3]^{2+}$/PEG_{3k}. Data presented as mean ± SD; *n*=3 experiments. (B) Confocal images (I row) of MoO_3-$[Ru(bpy)_3]^{2+}$ and (II row) MoO_3-$[Ru(bpy)_3]^{2+}$/PEG_{3k} labeled bEnd.3 cells.

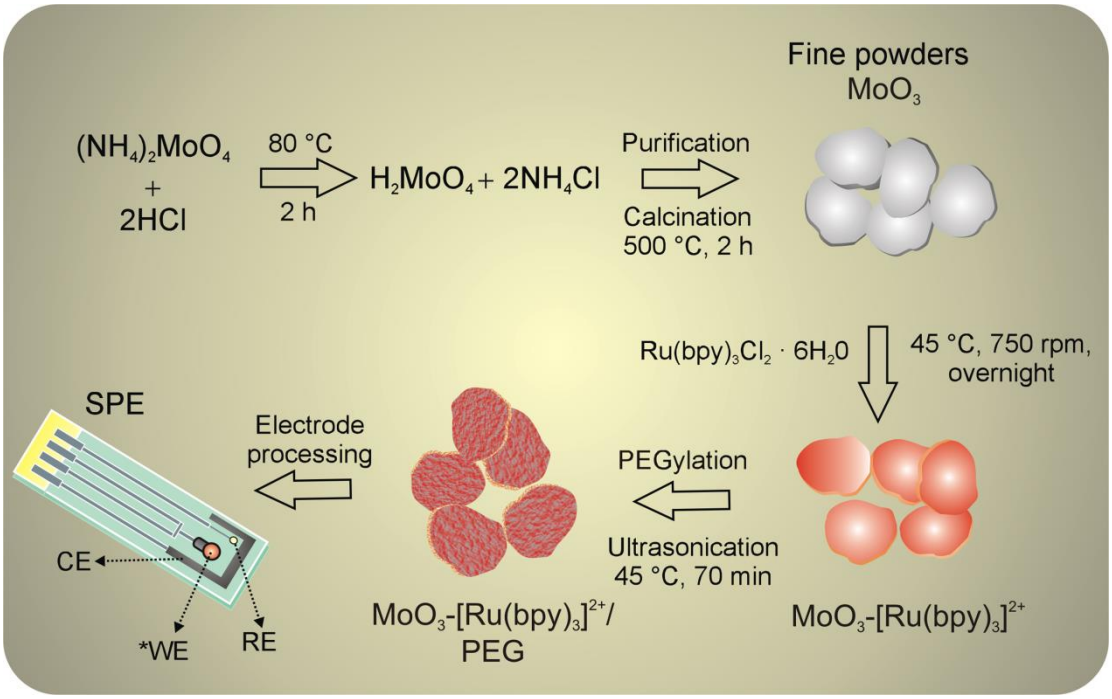

Scheme 1. Preparation of fine powders of MoO_3, functionalization with $[Ru(bpy)_3]^{2+}$, PEGylation and electrode processing using screen printed electrode (SPE). CE: counter electrode, RE: reference electrode and *WE: working electrode suitably modified with sheet-like structures of MoO_3 or MoO_3-$[Ru(bpy)_3]^{2+}$ or MoO_3-$[Ru(bpy)_3]^{2+}$ or MoO_3-$[Ru(bpy)_3]^{2+}$/PEG_{3k}.